Emulsifier Composition of Solid Lipid Nanoparticles (SLN) Affects Mechanical and Barrier Properties of SLN-Protein Composite Films

Verena Wiedenmann, Kathleen Oehlke, Ulrike van der Schaaf, Hanna M. Koivula, Kirsi S. Mikkonen, and Heike P. Karbstein

Abstract: Protein films can be applied to improve food quality and to reduce packaging waste. To overcome their poor water barrier properties, lipids are often incorporated. The function of incorporated lipid depends on the interface between filler and matrix. This study aimed to tailor the properties of a protein–lipid film by designing the oil/water interface to see if the concept of inactive/active filler is valid. Therefore, we varied the emulsifier stabilizing solid lipid nanoparticles (SLN) to promote (via β-lactoglobulin) or to minimize (via Tween 20) interactions between particle surface and protein. SLN were incorporated into protein films and film properties were determined. Addition of SLN led to significantly decreased water vapor permeability (WVP) of protein films. However, WVP was mainly affected by the emulsifiers and not by the lipid. Protein-stabilized SLN (BS) replaced a lacking protein in the protein network and therefore did not influence the mechanical properties of the films at ambient temperature. BS-composite films were temperature sensitive, as lipid and sucrose palmitate melted at temperatures above 40 °C. Tween 20-stabilized SLN (TS) led to reduced tensile strengths, probably due to perturbative effects of TS and plasticizing effects of Tween 20. Dynamic mechanical analysis showed that TS and Tween 20 increased film mobility. Melting of lipid and emulsifiers, and temperature-dependent behavior of Tween 20 led to a strong temperature dependence of the film stiffness. By designing the interface, particles can be used to tailor mechanical properties of protein films. Tuned edible films could be used to control mass transfers between foods.

Keywords: composite, edible coating, permeability, thermal properties, vapor transfer

Introduction

Using hydrocolloid films and coatings is a promising strategy to reduce packaging waste and to improve food quality. They can control mass transfers between foods, between food and its environment, and are often edible and degradable. The properties of edible protein films and coatings have been studied extensively recently (Chiralt, González-Martínez, Vargas, & Atarés, 2018; Wihodo & Moraru, 2013; Zink, Wyrobnik, Prinz, & Schmid, 2016). Whey protein isolate (WPI) films have proved to be good barriers against oxygen, but demonstrated low tensile strengths and poor moisture barriers because of their hydrophilic nature (Pérez-Gago, Nadaud, & Krochta, 1999). To overcome these shortcomings while maintaining the advantages of protein films, lipid components were added to increase the water vapor resistance of protein films. They can either be applied by coating the protein film or by incorporation of lipidic fillers such as oil droplets or fat particles (McHugh & Krochta, 1994; Shellhammer & Krochta, 1997; Sohail, Wang, Biswas, & Oh, 2006).

Tensile strength and water vapor permeability (WVP) were also improved by adding nanoscale and hydrophobic fillers (Kadam et al., 2013; Zhou, Wang, & Gunasekaran, 2009). The aspect ratio of nanoscale fillers is of great importance—the higher the aspect ratio of clay particles in polyimide-clay hybrid films, the better were the barrier properties and the storage moduli of films (Yano, Usuki, & Okada, 1997). In addition, the small size had a significant impact as it allowed a more homogenous distribution within the films and increased the protein–surface interactions. Strong protein–surface interactions have been reported to reinforce films efficiently (Huang, Xie, & Xiong, 2018; Pérez-Gago & Krochta, 2001). Tawakkal, Cran, and Bigger (2018) incorporated kenaf fiber to poly (lactic acid) composites. They found a significantly increased tensile strength if the fibers were treated prior to incorporation and explained this by increased adhesion between the treated fibers and the surrounding matrix. In protein gels, it is well known that added particles can reinforce, not influence at all or weaken the mechanical properties of the gels (Chen & Dickinson, 1999). Active fillers usually reinforce the mechanical strength of gels: Their surface interacts with the surrounding protein, leading to the incorporation of the particles within the gel network and thus supporting the network. In contrast, the surface of inactive fillers does not interact with the protein. Hence, they are inert fillers or can disturb the network formation, thereby resulting in weaker and less elastic gels. Therefore, modification of the surface of fillers to enhance interactions between particle and matrix seems promising to improve mechanical properties of protein films.

Solid lipid nanoparticles (SLN) are crystallized, nanoscaled lipid particles. They can be produced by crystallization of the lipid phase in oil-in-water nanoemulsions and typically consist of solid triglycerides, stabilized by one or more emulsifiers. In SLN, different lipid modifications can coexist, such as α-, β-,

JFDS-2019-0369 Submitted 3/14/2019, Accepted 10/15/2019. *Authors Wiedenmann and Oehlke are with Dept. of Food Technology and Bioprocess Engineering, Max Rubner-Institut, Federal Research Inst. of Nutrition and Food, Haid-und-Neu Str. 9, 76131 Karlsruhe, Germany. Authors Wiedenmann, van der Schaaf, and Karbstein are with Chair of Food Process Engineering, Inst. of Process Engineering in Life Sciences, Karlsruhe Inst. of Technology, Karlsruhe, Kaiserstr. 12, 76131 Karlsruhe, Germany. Authors Koivula and Mikkonen are with Dept. of Food and Environmental Sciences, Univ. of Helsinki, P.O. Box 27, 00014 Helsinki, Finland. Direct inquiries to author Oehlke (Email: kathleen.oehlke@mri.bund.de).*

Journal of Food Science A Publication of the Institute of Food Technologists

doi: 10.1111/1750-3841.14950

and β'-modification or supercooled melt. This leads to varying nanoparticle shapes, such as spheres or platelets (Mehnert & Mäder, 2012; Noack, Hause, & Mäder, 2012). In our previous work, we showed that triglyceride-based SLN are platelet shaped particles that do not agglomerate after protein addition (Milsmann, Oehlke, Schrader, Greiner, & Steffen-Heins, 2018). Furthermore, we showed that, depending on the emulsifier used, SLN can act as active or inactive filler and thus either reinforce or weaken a protein gel network (Wiedenmann et al., 2018).

On the basis of the above observations, several factors could make SLN efficient fillers for protein films: (1) The platelet-like shape and size of SLN, that is, the high aspect ratio and the large surface area that allow interactions with the protein. (2) The choice of emulsifier to stabilize the SLN either to promote or to prevent interactions between the particles' surface and the protein and thus determining the action mode as active or inactive filler. (3) The small size of SLN to ensure a homogeneous distribution and to increase the tortuosity in the continuous matrix. To our knowledge, there are no direct comparisons of active/inactive fillers in protein gels and the resulting films. We hypothesize that the concept of active/inactive fillers is also applicable on protein films. Therefore, the objective of this study was to investigate if the properties of protein films can be tailored by differently stabilized SLN, acting as active or inactive fillers. Thus, we dried the respective protein gels containing varying amounts of active, that is, protein-stabilized SLN or inactive, that is, Tween 20-stabilized SLN to produce films (Wiedenmann et al., 2018). To distinguish between the impact of the lipid particles themselves and the emulsifiers used to stabilize the particles, films containing only the mixture of emulsifiers but no lipid served as control.

Material and Methods

Material

β-Lactoglobulin (BLG) was isolated from BiPro whey protein isolate, kindly donated by Agropur Ingredients (Eden Prairie, MN, USA). Glyceryl tristearate and Tween 20® (Polyoxyethylene sorbitan monolaurate, Tween 20) was purchased from Sigma–Aldrich (St. Louis, MO, USA), Glucono-δ-lactone (GDL) and sucrose palmitate from Alfa Aesar (Karlsruhe, Germany). Soy lecithin "Emulpur IP" was kindly donated by Cargill (Cargill Texturizing Solutions, Hamburg, Germany). Potassium-di-hydrogen phosphate was purchased from Carl Roth GmbH (Karlsruhe, Germany), hydrochloric acid, sodium hydroxide, glycerol, and di-sodium hydrogen phosphate, calcium chloride from Merck KGaA (Darmstadt, Germany). All solutions were prepared in MilliQ water.

Purification of BLG. BLG was isolated from whey protein isolate (WPI), following a method described by Keppler, Sönnichsen, Lorenzen, and Schwarz, (2014) with slight modifications: 20% (w/w) WPI was dissolved in demineralized water and hydrated for 18 hr at 8 °C. Subsequently, the pH value was adjusted to 4.8 with hydrochloric acid to precipitate remaining caseins. Caseins were separated by centrifugation at 3,220 × g for 20 min. The pH value of the remaining protein solution was then set to 3.8 with hydrochloric acid and the solution was heated to 55 °C for 30 min. During this heat treatment, all whey proteins except BLG precipitated and were removed at 20 °C by centrifugation at 3,220 × g for 20 min. The pH value of the remaining supernatant was readjusted to 7.0 with sodium hydroxide before washing the protein three times with ultrapure water by ultrafiltration (Amicon Ultra-15, PLGC Ultracel-PL Membran MWCO of 10 kDa, Merck KGaA, Darmstadt, Germany). BLG solution was collected and freeze dried.

Table 1–Composition of the SLN and emulsifier mixtures (E) suspensions.

	TS	BS	E1	E2
Tristearin	5.0%	5.0%	–	–
Soy lecithin	0.25%	0.25%	0.25%	0.25%
Sucrose palmitate	1.51%	1.51%	1.51%	1.51%
Tween 20	4.0%	–	4.0%	–
BLG	–	0.5%	–	–

To check purity and denaturation degree of BLG, reversed phase-HPLC (Agilent 1290 Infinity LC System HPLC) was applied with a fluorescence detector and C-18 reversed-phase column (AerisTM XB-C18 Wide Pore 3.6 µm, 200 Å LC Column 50 × 2.1 mm, Phenomenex, Torrance, CA, USA).

Denaturation degree of BLG was determined using the respective German Industrial Standard procedure (DIN 10473). Samples were analyzed before and after a pH adjustment to 4.6 with hydrochloric acid. The concentrations of the supernatants were determined using following procedure: The injection volume was set to 10 µL at a flow rate of 1.2 mL/min and a column temperature of 40 °C. Eluents A (0.1% (v/v) trifluoroacetic acid (TFA) in water) and B (0.1% TFA (v/v) in acetonitrile) were used. Used elution gradient steps were 35% to 42.5% B (1 to 12.5 min), 42.5% to 46% B (12.5 to 20.5 min), 46% to 35% B (20.5 to 22 min), and 35% B (22 to 23 min). Fluorescence was monitored at excitation and emission wavelengths of 225 and 340 nm, respectively. BLG A and B appeared at about 15 and 14 min, respectively. No other peaks were detected. The degree of denaturation corresponded to the relative difference of the BLG concentration before and after precipitation due to pH adjustment and was below 1%.

SLN preparation. Tween 20- and protein-stabilized SLN were prepared by ultrasound-assisted hot emulsification as described by Wiedenmann et al. (2018). In brief, 0.125 g lecithin was added to 2.5 g of tristearin and heated to 80 °C. This temperature was held for at least 30 min to remove any crystal memory. A total of 22.375 g of 3.02% (w/w) sucrose palmitate in 5 mM phosphate buffer was added at 80 °C and immediately emulsified applying a sonicator (Branson Digital Sonifier, Emerson Industrial Automation, St. Louis, MO, USA) with a titanium tip at amplitude of 75% in pulsed mode (0.5 s on/off). To prepare Tween 20-stabilized SLN (TS), the hot emulsion was mixed with a hot (80 °C) 8% (w/w) Tween 20 solution in equal amounts and immediately cooled to 20 °C in ice water.

Protein-stabilized SLN (BS) were prepared by mixing one part emulsion at 60 °C and one part of a 1% (w/w) BLG solution (20 °C). The resulting emulsion was immediately cooled to 20 °C in ice water.

The prepared SLN were subsequently centrifuged at 3,170 × g for 10 min to remove any titanium that was abraded during sonication.

To prepare the emulsifier solutions, the respective amounts of emulsifier were dissolved in 5 mM phosphate buffer, heated at 80 °C for 20 min, and subsequently cooled down in ice water. Final composition of BS, TS, and emulsifier solutions are given in Table 1.

Size and zeta potential

Particle size and zeta potential (ZP) were analyzed using a ZetaSizer Nano ZS (Malvern Instruments, UK). ZPs were

Table 2–Film composition ([w:w], percentage in film forming solution or percentage in dry matter) of the different kinds of BLG-films; films were prepared with varying amounts of solid lipid nanoparticles (SLN) or emulsifiers (E), that were incorporated into the film forming solution. SLN were either stabilized by Tween 20 (TS) or by β-lactoglobulin (BS). Films without added emulsifier or SLN served as controls.

	In film forming solution			In dry mass						
	Protein solution*	SLN or E dispersion	Buffer solution	BLG**	Glycerol**	GDL	Tristearin	Tween 20	Sucrose palmitate	Lecithin
TS	50%	50%	0%	27.5%	13.8%	5.9%	24.6%	19.6%	7.4%	1.2%
TS	50%	25%	25%	37.4%	18.7%	8.0%	16.7%	13.4%	5.0%	0.8%
TS	50%	5%	45%	52.5%	26.2%	11.2%	4.7%	3.7%	1.4%	0.2%
TS	50%	2%	48%	55.8%	27.9%	12.0%	2.0%	1.6%	0.6%	0.1%
BS	50%	50%	0%	34.2%	17.1%	7.3%	30.6%	–	9.2%	1.5%
BS	50%	25%	25%	43.1%	21.6%	9.2%	19.3%	–	5.8%	1.0%
BS	50%	5%	45%	54.5%	27.2%	11.7%	4.9%	–	1.5%	0.2%
BS	50%	2%	48%	56.7%	28.4%	12.2%	2.0%	–	0.6%	0.1%
E1	50%	50%	0%	36.5%	18.2%	7.8%	–	26.0%	9.8%	1.6%
E2	50%	50%	0%	49.3%	24.6%	10.6%	–	–	13.3%	2.2%
Control	50%	–	50%	58.3%	29.2%	12.5%	–	–	–	–

*Protein concentration in the protein solution was set to 5.6% (w:v); **Glycerol:BLG ratio was kept constant (1:2);

measured via electrophoretic mobility. Prior to the measurements, the samples were diluted with MilliQ water to achieve a conductivity of 50 μS/cm. Particle sizes were analyzed using dynamic light scattering with a backscatter angle of 173°. We determined the *z*-averages based on the intensity-based particle size distributions using Mie theory. All measurements were performed at 25 °C.

Film preparation

Films with varying concentrations of SLN were produced. TS were incorporated after the heat treatment, as it is known that TS change their size during the heat treatment of the solution (Wiedenmann et al., 2018). Since BS were stabilized by untreated protein, the incorporation after the heat treatment of the protein would have resulted in a mixture of untreated and denatured protein. This would have caused overlapping effects, as both the kind of SLN and the ratio of untreated to denatured protein would influence the system. Hence, BS were added to the protein solution before the heat treatment. Films without SLN and films with only emulsifier solution but devoid of lipid served as controls.

To prepare protein films, we first produced cold-set gels according to Wiedenmann et al., 2018. In short, 5.6% BLG (v/w) was dissolved in 5 mM phosphate buffer, emulsifier solution (E2), or BS suspension at pH 7 and let hydrate for at least 18 hr at 5 °C. Subsequently, the protein solution was heated at 90 °C for 30 min to denature the protein. After heat treatment, the samples were cooled to 20 ± 1 °C in ice water. Before forming the gels, appropriate amounts of 5 mM buffer solution, TS suspension, or E1 solution were added yielding a final BLG concentration of 2.8%. Glycerin was added as plasticizer at a concentration of 1.4% (w/w; 50% of BLG). Gelation was subsequently induced by adding 0.6% (w/w) glucono-δ-lactone powder. The gels were cast in Teflon-coated Petri dishes. The total dry matter per area was 100 g/m^2 in all films to ensure a consistent film thickness. The gels were dried at 23 °C and 55% relative humidity (RH) and stored under these conditions for 6 days prior to film characterization. All films were prepared in triplicates. Final compositions of the films are presented in Table 2.

Haze

Haze measurements were performed in accordance to ASTM D1003-13 applying a spectrophotometer (uv-2501 PC, Shimadzu, Kyoto, Japan) coupled with a light trap of 150 mm diameter to trap the diffuse transmitted light. The values presented are the average of four measurements at a wavelength of 550 nm.

Moisture content and solubility

Squares of films with a side length of 2 cm were weighed and put on predried glass Petri dishes. Samples were dried at 100 °C for 20 hr and cooled in a desiccator prior to weighing again.

Solubility was determined by immersing squares of films (side length 2 cm) in 30 mL of MilliQ water. The samples were gently shaken for 24 hr at 25 °C and the films were subsequently dried at 100 °C for 24 hr. The solubility was calculated as follows:

$$\text{Solubility} = 100 - \frac{m_{\text{soaked, dried}}}{m_{\text{dry,initial}}} \times 100 \quad (1)$$

where $m_{\text{soaked, dried}}$ is the mass of the dried sample after soaking, whereas $m_{\text{dry, initial}}$ is the theoretical weight of the films after drying according to the respective measured moisture contents of the films.

Dynamic vapor sorption

A total of 10 to 15 mg of sample was weighed in a sample pan of a dynamic vapor sorption (DVS) intrinsic sorption microbalance (Surface Measurement Systems, Alperton, Middlesex, UK). The experiments were performed at 25 °C and relative humidity (RH) varied from 5% to 90%, increasing stepwise in 10% RH steps, except the first step, which was 5%. A step was finished after the sample was equilibrated at the respective RH. Subsequently, we calculated the water uptake applying following equation:

$$\text{Water uptake} = 100\frac{m_{moist} - m_{dry}}{m_{dry}} \quad (2)$$

where m_{moist} is the mass of the equilibrated sample at a chosen RH, whereas m_{dry} is the weight of the sample at 5% RH.

Mechanical properties

The elastic modulus, tensile strength, and elongation at break were determined for all films at 23 °C and 55% RH (climate room). An Instron 33R4465 universal testing machine with a load cell of 100 N was used. From three cast films of each type, 10 to 14 replicate specimens of a rectangular shape with the dimensions

of 5 mm × approximately 50 mm were tested. The thickness of the films was measured at four points using a micrometer (Lorentzen and Wettre, Kista Sweden, precision 0.001 mm) and averaged. The initial grip distance was set to 35 mm and the test speed was 10 mm/min.

Temperature and RH dependent dynamic mechanical analysis (DMA) was performed using a TA DMA Q 800 (New Castle, DE, USA). Film specimens had a width of 5.0 ± 0.2 mm. The gap between the clamps was set to 8.0 ± 0.2 mm. In all tests, the storage modulus (E') and loss modulus (E'') were recorded at an amplitude of 10 µm and a frequency of 1 Hz.

Temperature sweeps were conducted as follows: equilibration at 25 °C, cooling to –5 °C, isothermal treatment for 2 min, heating to 90 °C, and isothermal treatment 2 min. All temperature changes occurred at a rate of 2 °C/min.

For RH sweeps, films were conditioned as described by Mikkonen, Schmidt, Vesterinen, and Tenkanen (2013) by increasing the RH from 0% to 40% at a rate of 0.5%/min. Subsequently, the RH was decreased to 0% and kept for 30 min. Then, the RH was increased to 90% at 1%/5 min. During the RH-sweeps, the temperature was maintained at 25 °C.

Water vapor permeability

The WVP of all films was determined according to the ASTM E96/E96M-10 standard. An RH gradient of 0/75% was studied. Films were sealed in aluminium cups containing approximately 43 g of $CaCl_2$. An air gap of approximately 6 mm occurred between the salt and the underside of the films. The cups were placed in a desiccator cabinet. A fan circulated the air in the cabinets at a speed of 0.15 m/s and the temperature during the measurements was kept at 24 °C. Saturated NaCl solutions were used to maintain the RH at 75%.

The cups were weighed seven times in 2 days. Before each weighing, the exact temperature and RH in the cabinet was recorded using a Rotronic RH meter (Bassersdorf, Switzerland). A linear regression was made of the weight gain versus time. All regression lines had a R^2 of at least 0.98. By dividing the slopes by the film area, the water vapor transmission rate (WVTR) was calculated. We calculated the water vapor partial pressure at the underside of the films using the correction for resistance due to still air and specimen surface described in the ASTM E96/E96M-10. WVP was calculated by multiplying the WVTR by the thicknesses of the films and by dividing by the water vapor partial pressure difference between the both sides of the films. Three replicates of each film type were analyzed. Five points per films were analyzed regarding their thicknesses as described in section Mechanical properties and averaged.

Statistical analysis

All tests were performed at least three times if not stated otherwise. A one-way analysis of variance (ANOVA) was used to test the differences of the films applying OriginPro 2019. The Tukey's test was used as a post-hoc test for a pairwise comparison of the means. Samples were considered as statistically different at $P \leq 0.05$.

Results and Discussion

Characterization of SLN

Prior to incorporation, SLN were analyzed regarding their size, polydispersity index (PDI), and ZP (Table 3).

BS had a size of 129 ± 2 nm and exhibited a ZP of about –59 mV. TS were larger (156 ± 5 nm) and had a ZP of approximately –41 mV (Table 3). The PDI of TS and BS was below 0.3, indicating a narrow size distribution. These values are slightly larger than in earlier works (Wiedenmann et al., 2018), probably due to process variations.

Table 3–Size, polydispersity index (PDI), and zeta potential (ZP) of SLN that were either stabilized by β-lactoglobulin (BS) or Tween 20 (TS).

	z-Average	PDI	ZP
BS	129 ± 2 nm	0.17 ± 0.01	–59 ± 3 mV
TS	156 ± 5 nm	0.24 ± 0.02	–41 ± 3 mV

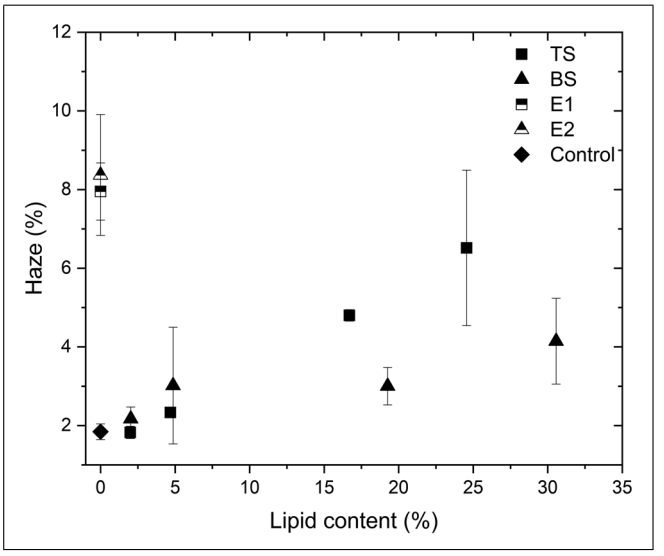

Figure 1–Haze indices of BLG-films, in which either Tween 20-stabilized SLN (TS) or protein-stabilized SLN (BS) were incorporated. As control served films without SLN or with the respective emulsifier mixture E1 (for TS) and E2 (for BS).

Appearance and haze

All obtained BLG films had a smooth surface without visible cracks and were easy to peel off from the casting plates. The films were flexible and almost transparent. Their haze indices are shown in Figure 1. The haze index gives information about irregularities in films that can occur during film formation, for examle, by particle agglomeration, cracks, or incompatibilities leading to phase separation. High surface roughness can also increase the haze of films (Azevedo et al., 2017; Billmeyer & Chen, 1985). Haze indices in dairy protein films were reported to be between 40% and 60% (Azevedo, Silva, Gonçalves Pereira, da Costa, & Borges, 2015; Sothornvit, Hong, An, & Rhim, 2010).

The haze indices increased with increasing content of TS, E1, or E2. BS had no significant effect on haze indices compared to the control. The low haze values for BS indicated a homogeneous network without any irregularities. We therefore concluded that BS did not cause defects within the network nor did they agglomerate during the film formation.

In contrast, TS increased the haze indices slightly. In previous work, we demonstrated that TS were inactive fillers and SEM-images revealed broken lamellae in protein gel networks (Wiedenmann et al., 2018). It is therefore likely, that the particles led to small internal defects within the film network or agglomerated. However, as the haze indices were still very low, we concluded that only few irregularities were present and both,

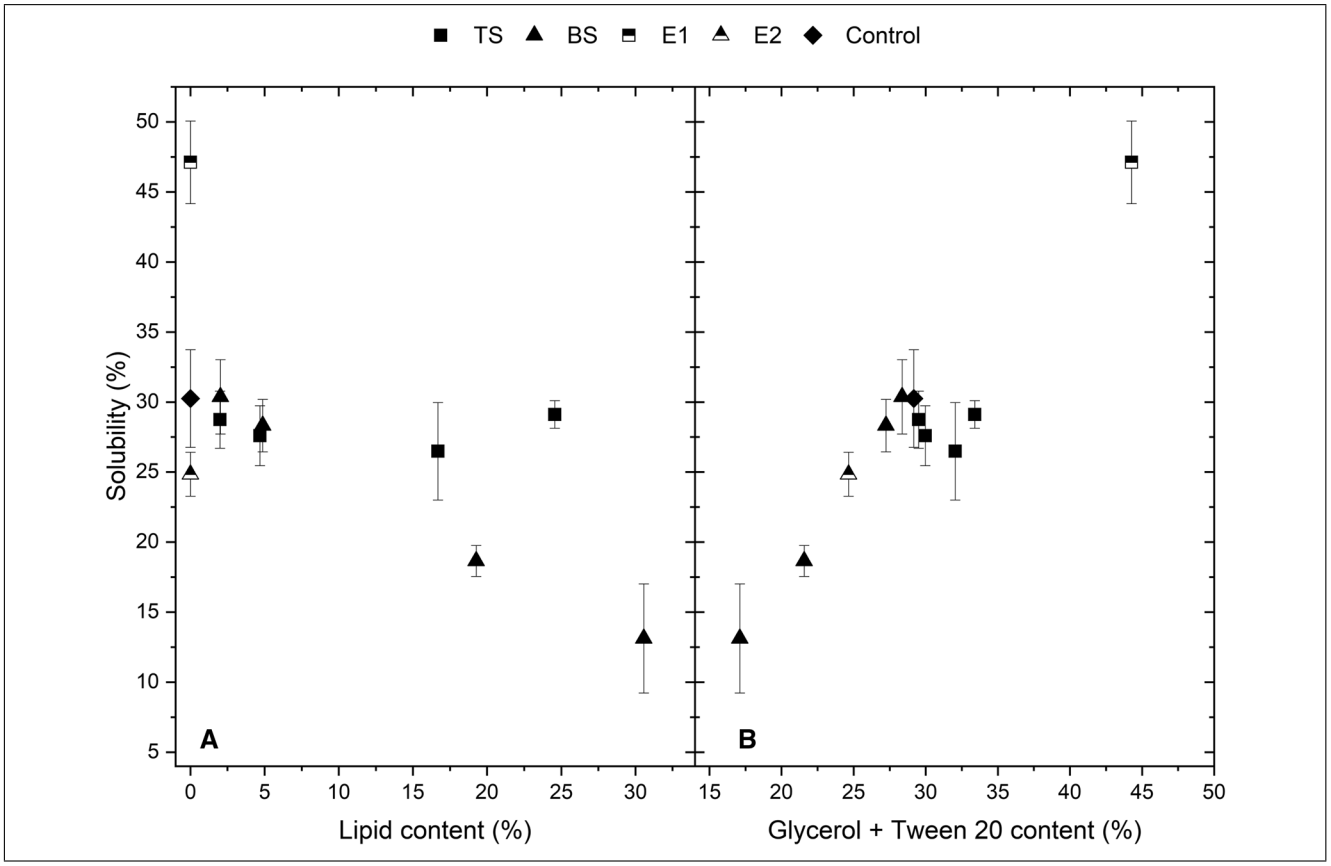

Figure 2–Solubility of different BLG-films in which we incorporated either Tween 20-stabilized SLN (TS) or protein-stabilized SLN (BS). Films without SLN or with the respective emulsifier mixtures served as control: E1 (for TS) and E2 (for BS). Solubility is presented as a function of the lipid content (A) or the glycerol and Tween 20 content (B).

active and inactive fillers, could be well incorporated in protein films without causing major defects.

Solubility

Film solubility can be an important property, whenever the film comes into contact with food containing high moisture contents or with water. In this study, all films maintained their integrity during the film solubility tests and could be removed from the liquid without breaking them. Obtaining intact films after soaking indicated that a stable protein network was obtained by the heat denaturation. Same observation has been reported by Pérez-Gago et al. (1999).

Films made from BLG showed a solubility of approximately 30% (Figure 2A). Increasing the content of BS decreased the solubility significantly. Fifty percent of BS resulted in about 50% of the solubility of the control film. In contrast, TS did not affect the solubility of the films compared to the control. Films that contained E1 resulted in an increased solubility. The presence of E2 did not cause a change in solubility compared to the control.

We propose that the dissolution of the films was mainly caused by the release of the water-soluble compounds, that is, glycerol and Tween 20. The amounts released correlate well with the added amounts of these components. This is visualized in Figure 2B. This phenomenon was already shown in WPI-films by other authors (Pérez-Gago et al., 1999; Ramos et al., 2013). Concluding, we could show that film solubility was controlled by soluble components of the films and not by particles interacting or not interacting with the surrounding protein matrix.

Water sorption

The shapes of all water sorption isotherms were typical for hydrophilic substances (Figure 3). The addition of SLN and the addition of emulsifiers resulted in a reduced moisture uptake of the films. All water sorption isotherms that were obtained experimentally were compared to the theoretical curves. For clarity, only the calculated curves of TS and of the control are presented in Figure 3. The calculation was carried out on the basis of the water uptake contribution of each raw material (Supporting Information). The water sorption correlated well with the BLG and glycerol content of the films, that is, the hydrophilic compounds (Figure 3, inset). We therefore propose that the reduced water sorption of E1/E2–BLG composite films was due to the lower amount of glycerol and protein. SLN-BLG-films absorbed less water than control films. Tristearin, E1, or E2 replaced part of the glycerol and protein (Table 2). In addition, tristearin did not contribute to the moisture absorption. The reduction of the moisture by the addition of SLN agreed well with the calculated adsorption based on the relative contribution of the components. This indicated that the water uptake was clearly dominated by the raw material and not by interactions between the substances.

Water vapor permeability

WVP is an important property of packaging films, as food quality loss can occur if moisture of the food is lost due to insufficient moisture retention by the packaging material.

The WVP of a film depends on its hydrophilicity as well as on cracks, irregularities, the type and amount of plasticizer, and on

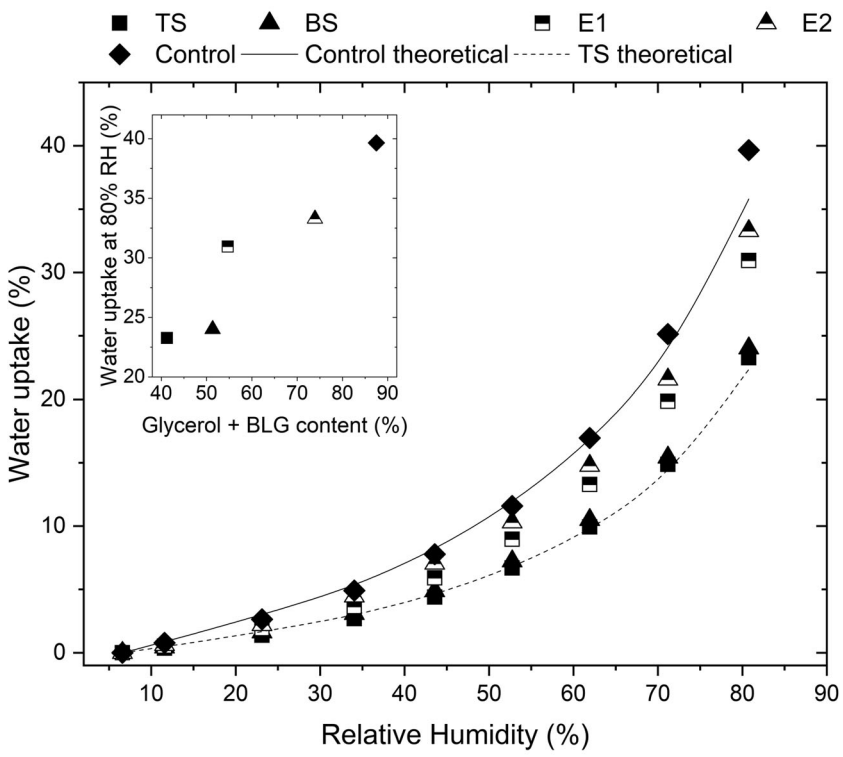

Figure 3–Water sorption and, as inlet, water uptake at 80% relative humidity of films in which we incorporated either Tween 20-stabilized SLN (TS) or protein-stabilized SLN (BS). Films without SLN or with the respective emulsifier mixtures E1 (for TS) and E2 (for BS) served as control.

the steric hindrance in the film structure. We proposed that the addition of SLN to BLG films would reduce their hydrophilicity thereby reducing the WVP. We further hypothesized that active fillers would lead to a more homogeneous and denser network in composite films and hence decrease the WVP. With inactive fillers, irregularities and broken lamellae would occur, which would increase the WVP.

WPI and BLG are known to be hydrophilic because of their highly polar groups. WPI and BLG films therefore generally show high WVP. This was also reflected in our results with WVP of up to 260 $\frac{\text{g mm}}{\text{m}^2 \text{ day kPa}}$ (Figure 4). The incorporation of both kinds of SLN decreased the WVP with increasing concentration of SLN. The addition of the highest amount of SLN resulted in a decrease of the WVP to approximately 50 $\frac{\text{g mm}}{\text{m}^2 \text{ day kPa}}$. Also, the incorporation of E1 and E2 resulted in a significant decrease in WVP. No difference between the WVP of films with E1 or E2 could be observed.

Tristearin has a very hydrophobic nature and, as present in SLN, appeared as particles. Particles can reduce the hydrophilicity of films and also increase the permeation distance for water vapor through a protein film. At similar lipid contents, TS decreased the WVP more efficiently than BS (Figure 4). However, the lipid content was accompanied by different types and amounts of emulsifiers, and their role should also be considered. This becomes very clear for films containing E1 or E2: Those films showed the lowest WVP of all films (Figure 4). Emulsifiers are generally known to reduce the WVP in biopolymer films as they contain hydrophobic regions (Andreuccetti, Carvalho, Galicia-García, Martínez-Bustos, & Grosso, 2011; Bravin, Peressini, & Sensidoni, 2004; Jongjareonrak, Benjakul, Visessanguan, & Tanaka, 2006). These hydrophobic regions reduce the hydrophilicity of films and, at the same time, the emulsifiers are very homogeneously dispersed. This is pointed out in Figure 4B. Comparison of films containing E1 and E2 leads to the conclusion that sucrose palmitate reduced the WVP more efficiently than E1. Hence, the different reduction in WVP caused by TS and BS could be related to the emulsifiers present.

The WVP of conventional plastic films (LDPE, HDPEE, PP, PET, PS, PVOH, EVA, PVC, or PA) are below 1 $\frac{\text{g mm}}{\text{m}^2 \text{ day kPa}}$ (Bastarrachea, Dhawan, & Sablani, 2011). The BLG-films had considerably higher WVP, also at the highest amounts of emulsifiers and lipid particles.

In conclusion, we could show that the WVP of protein films was mainly affected by incorporated emulsifiers and not by the way SLN are incorporated in the network, that is, as active or inactive fillers.

Tensile properties

If protein films are to be used as packaging material, they must withstand a certain stress that could occur during handling or processing. To describe the mechanical properties of the films, elastic modulus (E), tensile strength, and elongation at break were determined for all films. Values for elongation at break can be found in the Supporting Information.

Values for E, tensile strength, and elongation at break of all films were in the range of 60 to 200 MPa, 1 to 5 MPa, and 10% to 60%, respectively (Figure 5; Supporting Information). The values are within the range typically reported for WPI films (Pérez-Gago et al., 1999; Sothornvit & Krochta, 2001). BS had no impact on the mechanical properties of the BLG films, whereas TS weakened the films: E and the tensile strength decreased significantly with increasing content of TS. The addition of E1 to the film forming solution resulted in a reduced E and tensile strength of the produced films. If the film composition included E2, E and tensile strength decreased as well, but to a lesser extent.

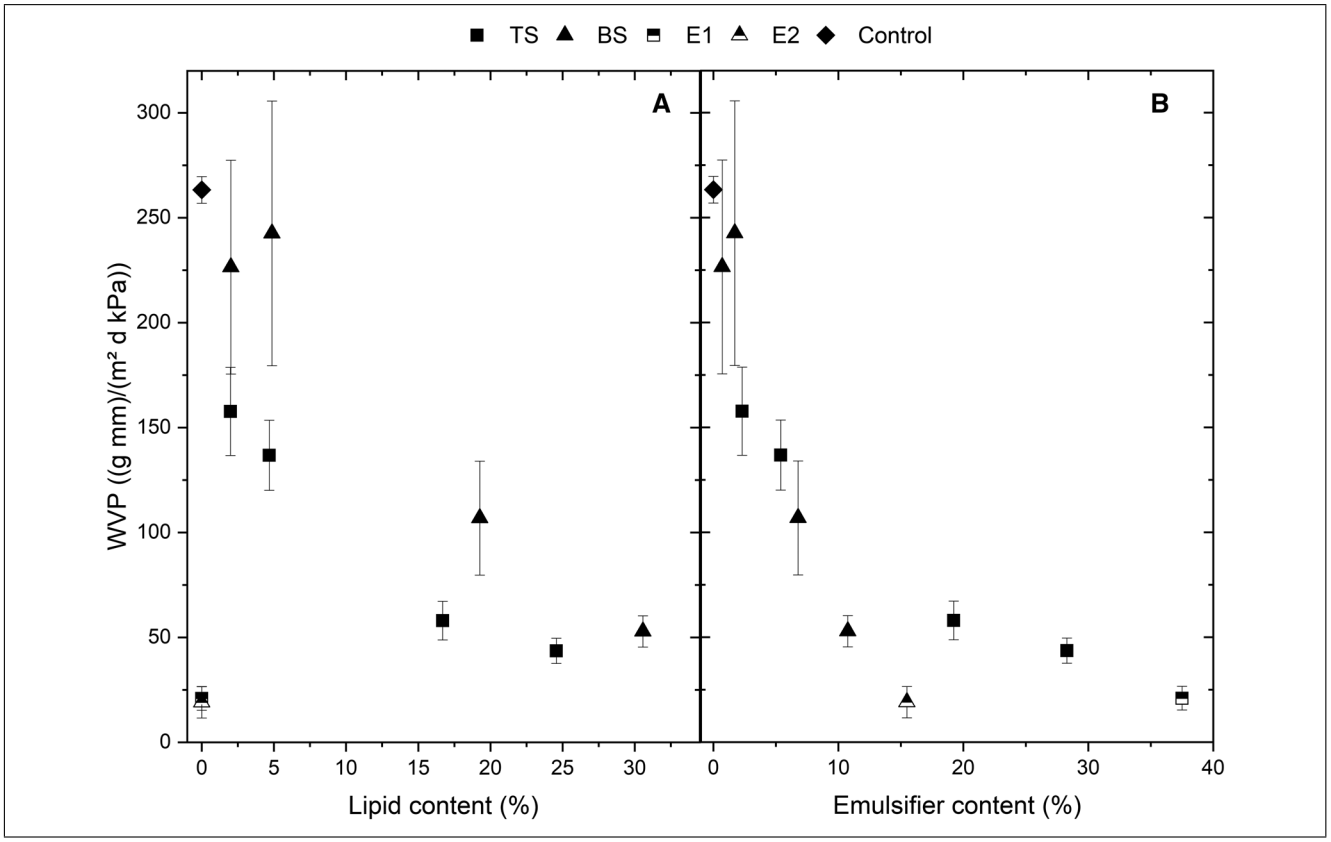

Figure 4–Water vapor permeability of BLG-films, in which we incorporated either Tween 20-stabilized SLN (TS) or protein-stabilized SLN (BS). Films without SLN or with the respective emulsifier mixtures E1 (for TS) and E2 (for BS) served as control. The results are presented as a function of the total lipid content (A) or total content of emulsifier (B).

The mechanical properties of the films are mainly influenced by the film building polymer, which was the protein. During the film forming, the protein formed a three-dimensional network that constitutes a self-standing film after drying. The density of this protein network was responsible for the strength of the film. All films were prepared with the same thickness, that is, with the same amount of dry mass per area. By adding lipids and emulsifiers, the percentage of the protein per area and thus the protein density in the films was reduced. We expected BS to be incorporated into the protein network and hence to be a part of the structure. As the replacement of protein by BS did not affect the tensile properties of BLG films, we conclude that they acted as active fillers in protein films, and therefore were part of the network. This behavior has been described for BS in protein gels before (Wiedenmann et al., 2018).

In contrast, TS acted as inactive filler in protein gels, leading to incomplete pores and thus weakened the mechanical properties of protein gels (Wiedenmann et al., 2018). Likewise, the resulting TS enriched films had lower E and tensile strength.

Films were significantly weaker in the presence of E1, i.e., in the presence of high amounts of Tween 20. Tween 20 is a small surfactant that can fit between the BLG molecules or interfere interactions between them, leading to a higher molecular mobility. In this way, Tween 20 could act as plasticizer. The plasticizing effect of Tween 20 is also reported elsewhere (Rodríguez, Osés, Ziani, & Maté, 2006; Ziani, Oses, Coma, & Maté, 2008).

Values for tensile moduli of conventional plastic films typically are in the range of 0.2 to 3.5 GPa, the tensile strengths are between 6 and 177 MPa, and elongations at break between 10% and 1,000% (Bastarrachea et al., 2011). Thus, the BLG-films in the presence of SLN or emulsifiers were weaker compared to conventional plastics.

In summary, the weakening of protein films by incorporation of inactive fillers was probably due to overlapping effects of Tween 20 as plasticizer and an incomplete network caused by the inactive fillers. BS, on the other hand, acted as active filler and did therefore not influence the mechanical properties.

Dynamic mechanical analysis

As active/inactive particles as well as the added emulsifiers can be expected to affect the melting point and molecular mobility of the systems, we performed dynamic mechanical analysis as a function of the temperature and the relative humidity (RH).

BLG films, in which the highest amount of TS was incorporated, showed the lowest stiffness of all films studied (Figure 6A) as indicated by a low storage modulus over temperature. E1, E2, and BS reduced the stiffness of the films to a lesser degree (Figure 6A and 6C).

We could not observe glass-transition in any of the films under the experimental conditions because the storage modulus exhibited no maxima. However, slope changes occurred at several temperatures. These changing points at intermediate temperatures indicated transitions that may correspond to either reconfiguration of the BLG-network or changes on the molecular level, such as changes in conformation of the protein or melting of lipids or emulsifiers (Bonnaillie & Tomasula, 2015).

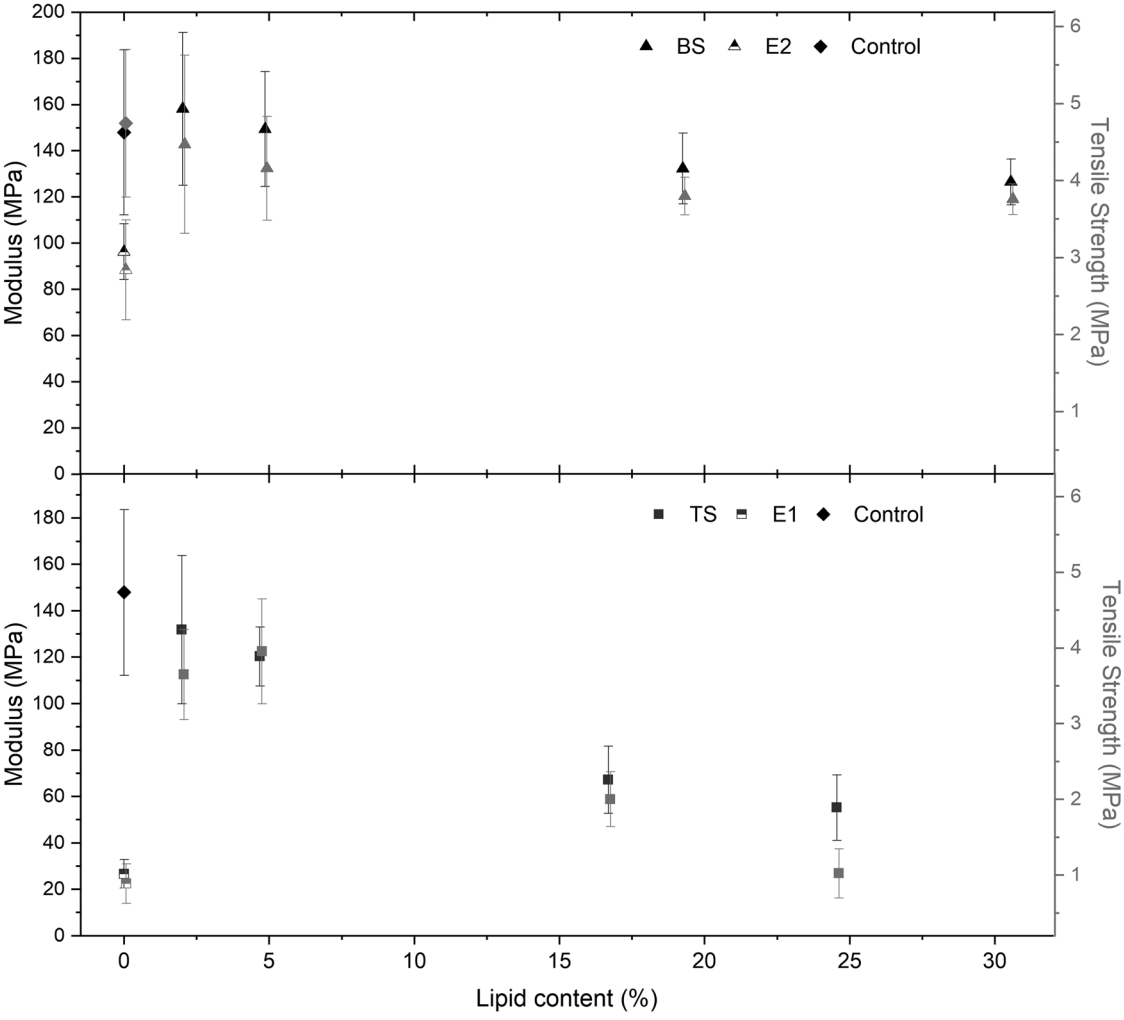

Figure 5–Elastic Modulus, and tensile strength of BLG films in which we incorporated either protein-stabilized SLN (BS, upper figure) or Tween 20-stabilized SLN (TS, lower figure). Films without SLN or with the respective emulsifier mixtures E1 (for TS) and E2 (for BS) served as control.

Above 0 °C, the storage moduli (E') of all films decreased with increasing temperature (Figure 6A and 6C). This decrease indicated a loss of elasticity as well as a loss of resistance to plastic deformation. To allow a better comparison of the curve shapes, we defined E^*_{rel} as E' by E‘ at the lowest temperature for each film (Figure 6B and 6C).

Films containing TS, the inactive filler, showed a pronounced decrease of E^*_{rel} compared to the control above a temperature of about 40 °C as indicated by a lower curve of the relative storage modulus. At a temperature of about 60 to 65 °C, a strong drop of E^*_{rel} was observed. At temperatures above 75 to 80 °C, films containing E1 or high TS contents showed values for E^*_{rel} close to zero. All these events were more pronounced with increasing TS, and thus increasing emulsifier contents.

Tween 20 and sucrose palmitate stabilized SLN exhibited a melting range from around 45 °C to about 60 °C (Oehlke, Behsnilian, Mayer-Miebach, Weidler, & Greiner, 2017). Liquid droplets show reduced stiffness compared to solid particles, thus they weaken the network. Therefore, it is likely that the melting of the lipid was responsible for the more pronounced decline of E^*_{rel} of the composite films at temperatures above 40 °C compared to the control. However, also the film containing E1 showed a strong decrease of E^*_{rel} at temperatures above 65 °C and the curves showed no shoulder-like peak. Temperature-dependent properties of Tween 20 could have led to this film behavior. Tween 20 has a cloud point around 40 to 80 °C depending on its concentration, on the solvent, and on further substances (Chawla & Mahajan, 2011). However, film weakening because of the cloud point has not yet been reported.

In the films containing BS, we could observe a drop of E^*_{rel} at temperatures above 40 °C compared to the control, followed by a shoulder-like peak at about 70 °C (Figure 6D). With increasing content of SLN, the drop of the E^*_{rel} was more pronounced. It is likely that BS melted around these temperatures, leading to weaker films. However, also films containing only E2 but no lipid showed a more pronounced shouldering around 45 °C compared to the control films. Sucrose palmitate has a melting point of around 45 °C, and we think that this melting event led to an increased E^*_{rel} of films containing E2.

The more pronounced weakening of films by the incorporation of TS compared to BS is in good accordance with the tensile properties of the films (section "Tensile properties") and was an effect of the active/inactive filler characteristics and plasticizing effects of Tween 20.

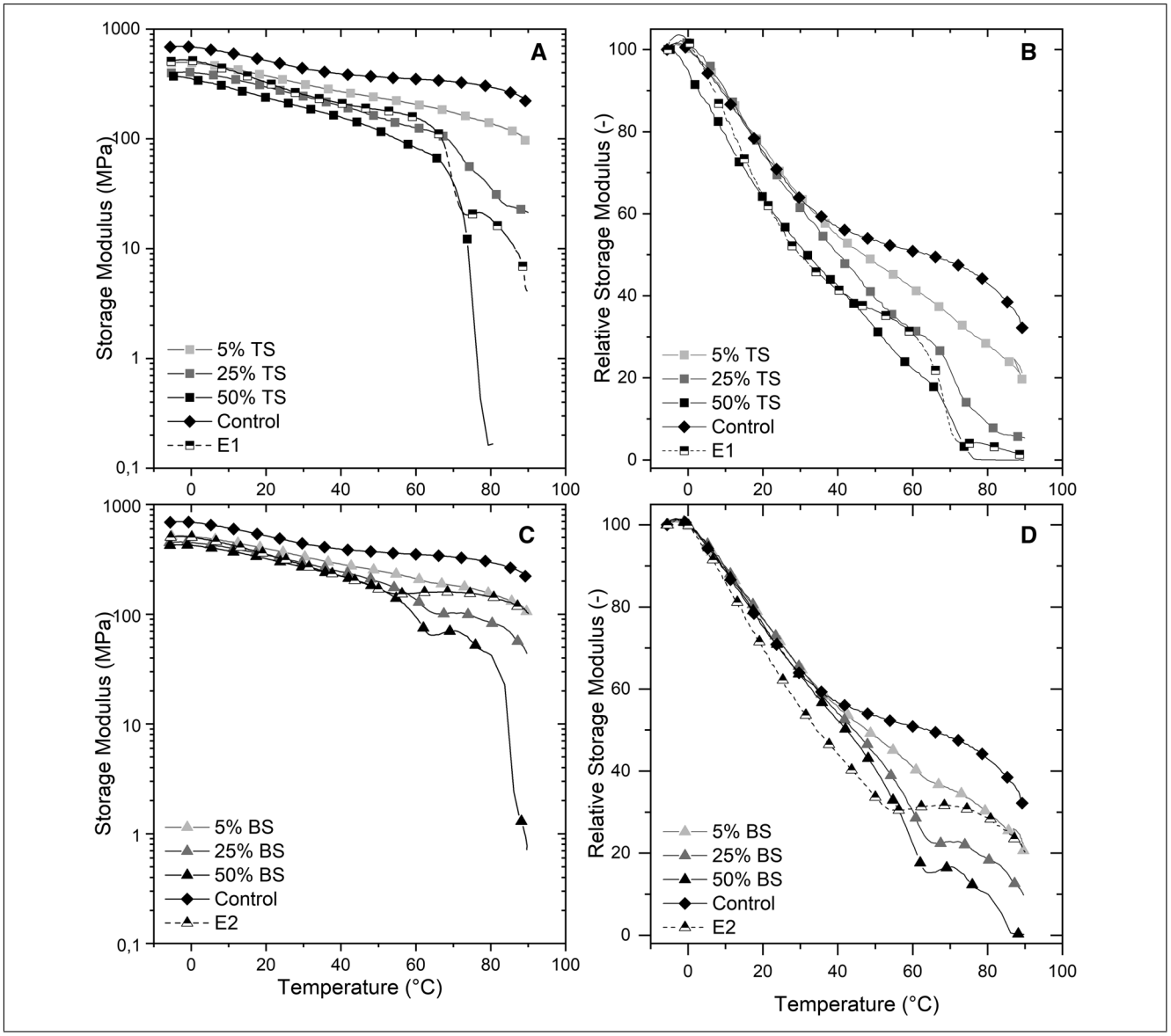

Figure 6–Storage modulus of films as a function of the temperature. (A) and (B) are the films with BLG stabilized SLN (BS) and (C) and (D) the films with Tween 20 stabilized SLN (TS), with the respective emulsifiers E1 or E2 incorporated. To better compare the shape of the curves, (B) and (D) represent the relative storage modulus of the films.

With increasing humidity, both E' and E'' of all films decreased (Figure 7; Supporting Information). The films softened as they absorbed water, leading to rearrangement of protein, emulsifiers, and other molecules. Water clearly acted as plasticizer and loosened the structure, thus reducing the stiffness of BLG films (Escalante et al., 2012). Values of tan δ stagnated in all films at low RH. However, at RH of about 50% to 55%, the slope of increasing tan δ of all films steepened. This first transition was probably due to critical water content inside the films, leading to the reconfiguration of the BLG molecules or the BLG/glycerol/water network. This led to a looser structure, allowing the molecules to absorb even more water (Bonnaillie & Tomasula, 2015). Another transition humidity, indicated by the peak of tan δ, was observed at RH of 75% to 87%. This can also be explained by interactions between adsorbed water and the film. These interactions may have caused an increased molecular mobility of the protein, thus allowing a further reconfiguration or reorganization of the molecules or aggregates in the film network in a way that occurred as film softening and a peak of tan δ. This last transition RH increased depending on the additives in the order TS<E1<E2≈BS≈control. The lower transition RH of TS and E1 samples could be attributed to a lower interaction between the network forming molecules in the film containing inactive fillers or Tween 20. Thus, higher molecular mobility occurred that could have caused the decreased rigidity of the film structure. The lower interactions could have increased the water adsorption and hence increased the plasticizing effect of water in the films. However, in DVS measurements, we could not see increased water absorption at 80% RH for TS and BS films (section "Water sorption"). We therefore suggest that the inactive filler particles and Tween 20 caused the increased mobility within the films, enabling and/or facilitating interactions between water and the hydrophilic regions of the protein. Lower humidity was therefore necessary to lead to a looser structure as reported for xylan films (Escalante et al., 2012).

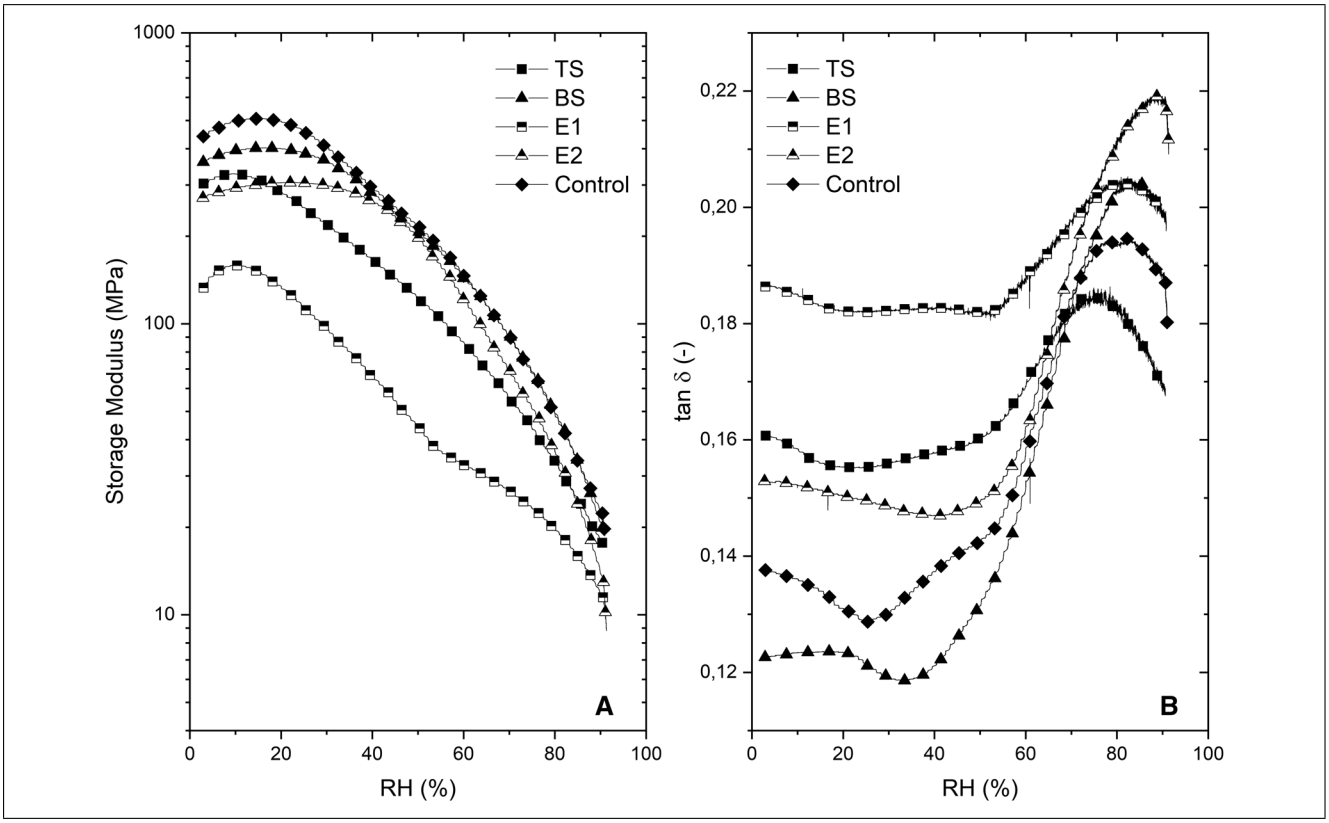

Figure 7–Storage modulus and tan δ as a function of the relative humidity (RH%) for the films, in which SLN and emulsifier were incorporated.

In conclusion, we could observe that the addition of the inactive filler TS led to lower stiffness within protein films. Especially the emulsifier Tween 20 seemed to have a great impact on the molecular mobility of the films and to have reduced interacting forces. The melting of film components and temperature-dependent behavior of Tween 20 led to a strong temperature dependence of all films.

Conclusion

BLG films enriched with different amounts of active or inactive fillers were prepared. Protein-stabilized solid lipid nanoparticles (BS) served as active filler, Tween 20-stabilized SLN were inactive fillers. The films were characterized regarding their haze, solubility, water uptake, water vapor permeability, and mechanical properties.

Films free from irregularities could be successfully prepared containing both active and inactive fillers. WVP properties of protein films were mainly affected by the emulsifiers and not by the active or inactive fillers. Inactive fillers led to reduced mechanical strength of the films. This was probably due to overlapping effects of a weakened protein network and plasticizing effects of Tween 20. The melting of tristearin and sucrose palmitate as well as temperature-dependent behavior of Tween 20 led to a strong temperature dependence of all films.

The active filler BS, on the other hand, did not influence the mechanical properties of the films at ambient temperatures. However, the melting of tristearin and sucrose palmitate led to temperature sensitive films.

The concept of active/inactive filler as a tool to impact protein matrices in a targeted way is also valid in protein films. Plasticizer and particles (active/inactive) contribute differently to film properties. Film properties can thus be tailored by choosing differently stabilized SLN and/or emulsifiers. This study advances sustainable food packaging and/or novel material development by enabling the production of protein films with tailored characteristics to reduce food quality losses.

Acknowledgments

The authors thank Zeynep Tacer-Caba for their fruitful discussion and excellent help. This work was supported by funds of the Karlsruhe House of Young Scientists (KHYS), and the Federal Ministry of Food and Agriculture (BMEL) based on a decision of the Parliament of the Federal Republic of Germany via the Federal Office for Agriculture and Food (BLE) under the innovation support program.

Author Contributions

Experiments were designed by V. Wiedenmann, K. Oehlke, U. van der Schaaf, H. Kiovula, K. Mikkonen, and H. Karbstein. Data were collected by V. Wiedenmann. The experimental results were interpreted by V. Wiedenmann, K. Oehlke, U. van der Schaaf, H. Kiovula, K. Mikkonen, and H. Karbstein. The manuscript was written by V. Wiedenmann. All authors discussed the results, contributed to the final manuscript, and approved it.

Conflicts of Interest

The authors declare no conflict of interest.

References

Andreuccetti, C., Carvalho, R. A., Galicia-García, T., Martínez-Bustos, F., & Grosso, C. R. F. (2011). Effect of surfactants on the functional properties of gelatin-based edible films. *Journal of Food Engineering*, *103*(2), 129–136. https://doi.org/10.1016/j.jfoodeng.2010.10.007

ASTM E96/E96M-10, Standard Test Methods for Water Vapor Transmission of Materials, ASTM International, West Conshohocken, PA, 2010, https://doi.org/10.1520/E0096_E0096M-10

ASTM D1003-13, Standard Test Method for Haze and Luminous Transmittance of Transparent Plastics, ASTM International, West Conshohocken, PA, 2013, https://doi.org/10.1520/D1003-13

Azevedo, V. M., Dias, M. V., Borges, S. V., Fernandes, R. V. d. B., Silva, E. K., Medeiros, É. A., & Ferreira Soares, N. d. F. (2017). Optical and structural properties of biodegradable whey protein isolate nanocomposite films for active packaging. *International Journal of Food Properties*, *20*(sup2), 1869–1878. https://doi.org/10.1080/10942912.2017.1354883

Azevedo, V. M., Silva, E. K., Gonçalves Pereira, C. F., da Costa, J. M. G., & Borges, S. V. (2015). Whey protein isolate biodegradable films: Influence of the citric acid and montmorillonite clay nanoparticles on the physical properties. *Food Hydrocolloids*, *43*, 252–258. https://doi.org/10.1016/j.foodhyd.2014.05.027

Bastarrachea, L., Dhawan, S., & Sablani, S. S. (2011). Engineering Properties of Polymeric-Based Antimicrobial Films for Food Packaging: A Review. *Food Engineering Reviews*, *3*(2), 79–93. https://doi.org/10.1007/s12393-011-9034-8

Billmeyer, F. W., & Chen, Y. (1985). On the measurement of haze. *Color Research & Application*, *10*(4), 219–224. https://doi.org/10.1002/col.5080100410

Bonnaillie, L. M., & Tomasula, P. M. (2015). Application of humidity-controlled dynamic mechanical analysis (DMA-RH) to moisture-sensitive edible casein films for use in food packaging. *Polymers*, 7(1), 91.

Bravin, B., Peressini, D., & Sensidoni, A. (2004). Influence of emulsifier type and content on functional properties of polysaccharide lipid-based edible films. *Journal of Agricultural and Food Chemistry*, *52*(21), 6448–6455. https://doi.org/10.1021/jf040065b

Chawla, J., & Mahajan, R. K. (2011). Cloud point studies of Tween and glycol in the presence of salts. *Journal of Dispersion Science and Technology*, *32*(6), 822–827. https://doi.org/10.1080/01932691.2010.488138

Chen, J., & Dickinson, E. (1999). Effect of surface character of filler particles on rheology of heat-set whey protein emulsion gels. *Colloids and Surfaces B: Biointerfaces*, *12*(3–6), 373–381. https://doi.org/10.1016/S0927-7765(98)00091-5

Chiralt, A., González-Martínez, C., Vargas, M., & Atarés, L. (2018). 18 - Edible films and coatings from proteins. In R. Y. Yada (Ed.), *Proteins in Food Processing (Second Edition)* (pp. 477–500). Sawston, UK: Woodhead Publishing.

Escalante, A., Gonçalves, A., Bodin, A., Stepan, A., Sandström, C., Toriz, G., & Gatenholm, P. (2012). Flexible oxygen barrier films from spruce xylan. *Carbohydrate Polymers*, *87*(4), 2381–2387. https://doi.org/10.1016/j.carbpol.2011.11.003

Huang, X., Xie, F., & Xiong, X. (2018). Surface-modified microcrystalline cellulose for reinforcement of chitosan film. *Carbohydrate Polymers*, *201*, 367–373. https://doi.org/10.1016/j.carbpol.2018.08.085

Jongjareonrak, A., Benjakul, S., Visessanguan, W., & Tanaka, M. (2006). Fatty acids and their sucrose esters affect the properties of fish skin gelatin-based film. *European Food Research and Technology*, *222*(5), 650–657. https://doi.org/10.1007/s00217-005-0151-6

Kadam, D. M., Thunga, M., Wang, S., Kessler, M. R., Grewell, D., Lamsal, B., & Yu, C. (2013). Preparation and characterization of whey protein isolate films reinforced with porous silica coated titania nanoparticles. *Journal of Food Engineering*, *117*(1), 133–140. https://doi.org/10.1016/j.jfoodeng.2013.01.046

Keppler, J. K., Sönnichsen, F. D., Lorenzen, P.-C., & Schwarz, K. (2014). Differences in heat stability and ligand binding among β-lactoglobulin genetic variants A, B and C using 1H NMR and fluorescence quenching. *Biochimica et Biophysica Acta (BBA) - Proteins and Proteomics*, *1844*(6), 1083–1093. https://doi.org/10.1016/j.bbapap.2014.02.007

McHugh, T. H., & Krochta, J. M. (1994). Water vapor permeability properties of edible whey protein-lipid emulsion films. *Journal of the American Oil Chemists' Society*, *71*(3), 307–312. https://doi.org/10.1007/bf02638058

Mehnert, W., & Mäder, K. (2012). Solid lipid nanoparticles. *Advanced Drug Delivery Reviews*, *64*, 83–101. https://doi.org/10.1016/j.addr.2012.09.021

Mikkonen, K. S., Schmidt, J., Vesterinen, A.-H., & Tenkanen, M. J. J. o. M. S. (2013). Crosslinking with ammonium zirconium carbonate improves the formation and properties of spruce galactoglucomannan films. *Journal of Materials Science*, *48*(12), 4205–4213. https://doi.org/10.1007/s10853-013-7233-9

Milsmann, J., Oehlke, K., Schrader, K., Greiner, R., & Steffen-Heins, A. (2018). Fate of edible solid lipid nanoparticles (SLN) in surfactant stabilized o/w emulsions. Part 1: Interplay of SLN and oil droplets. *Colloids and Surfaces A: Physicochemical and Engineering Aspects*, *558*, 615–622. https://doi.org/10.1016/j.colsurfa.2017.05.073

Noack, A., Hause, G., & Mäder, K. (2012). Physicochemical characterization of curcuminoid-loaded solid lipid nanoparticles. *International Journal of Pharmaceutics*, *423*(2), 440–451. https://doi.org/10.1016/j.ijpharm.2011.12.011

Oehlke, K., Behsnilian, D., Mayer-Miebach, E., Weidler, P. G., & Greiner, R. (2017). Edible solid lipid nanoparticles (SLN) as carrier system for antioxidants of different lipophilicity. *PLoS One*, *12*(2), e0171662. https://doi.org/10.1371/journal.pone.0171662

Pérez-Gago, M. B., & Krochta, J. M. (2001). Lipid Particle Size Effect on Water Vapor Permeability and Mechanical Properties of Whey Protein/Beeswax Emulsion Films. *Journal of Agricultural and Food Chemistry*, *49*(2), 996–1002. https://doi.org/10.1021/jf000615f

Pérez-Gago, M. B., Nadaud, P., & Krochta, J. M. (1999). Water Vapor Permeability, Solubility, and Tensile Properties of Heat-denatured versus Native Whey Protein Films. *Journal of Food Science*, *64*(6), 1034–1037. https://doi.org/10.1111/j.1365-2621.1999.tb12276.x

Ramos, Ó. L., Reinas, I., Silva, S. I., Fernandes, J. C., Cerqueira, M. A., Pereira, R. N., . . . Malcata, F. X. (2013). Effect of whey protein purity and glycerol content upon physical properties of edible films manufactured therefrom. *Food Hydrocolloids*, *30*(1), 110–122. https://doi.org/10.1016/j.foodhyd.2012.05.001

Rodríguez, M., Osés, J., Ziani, K., & Maté, J. I. (2006). Combined effect of plasticizers and surfactants on the physical properties of starch based edible films. *Food Research International*, *39*(8), 840–846. https://doi.org/10.1016/j.foodres.2006.04.002

Shellhammer, T. H., & Krochta, J. M. (1997). Whey protein emulsion film performance as affected by lipid type and amount. *Journal of Food Science*, *62*(2), 390–394. https://doi.org/10.1111/j.1365-2621.1997.tb04008.x

Sohail, S. S., Wang, B., Biswas, M. A. S., & Oh, J.-H. (2006). Physical, Morphological, and Barrier Properties of Edible Casein Films with Wax Applications. *Journal of Food Science*, *71*(4), C255–C259. https://doi.org/10.1111/j.1750-3841.2006.00006.x

Sothornvit, R., Hong, S.-I., An, D. J., & Rhim, J.-W. (2010). Effect of clay content on the physical and antimicrobial properties of whey protein isolate/organo-clay composite films. *LWT - Food Science and Technology*, *43*(2), 279–284. https://doi.org/10.1016/j.lwt.2009.08.010

Sothornvit, R., & Krochta, J. M. (2001). Plasticizer effect on mechanical properties of β-lactoglobulin films. *Journal of Food Engineering*, *50*(3), 149–155. https://doi.org/10.1016/S0260-8774(00)00237-5

Tawakkal, I. S. M. A., Cran, M. J., & Bigger, S. W. (2018). The influence of chemically treated natural fibers in poly(lactic acid) composites containing thymol. *Polymer Composites*, *39*(4), 1261–1272. https://doi.org/10.1002/pc.24062

Wiedenmann, V., Oehlke, K., van der Schaaf, U., Hetzer, B., Greiner, R., & Karbstein, H. P. (2018). Impact of the incorporation of solid lipid nanoparticles on β-lactoglobulin gel matrices. *Food Hydrocolloids*, *84*, 498–507. https://doi.org/10.1016/j.foodhyd.2018.06.007

Wihodo, M., & Moraru, C. I. (2013). Physical and chemical methods used to enhance the structure and mechanical properties of protein films: A review. *Journal of Food Engineering*, *114*(3), 292–302. https://doi.org/10.1016/j.jfoodeng.2012.08.021

Yano, K., Usuki, A., & Okada, A. (1997). Synthesis and properties of polyimide-clay hybrid films. *Journal of Polymer Science Part A: Polymer Chemistry*, *35*(11), 2289–2294. https://doi.org/10.1002/(SICI)1099-0518(199708)35:11<2289::AID-POLA20>3.0.CO;2-9

Zhou, J. J., Wang, S. Y., & Gunasekaran, S. (2009). Preparation and Characterization of Whey Protein Film Incorporated with TiO2 Nanoparticles. *Journal of Food Science*, *74*(7), N50–N56. https://doi.org/10.1111/j.1750-3841.2009.01270.x

Ziani, K., Oses, J., Coma, V., & Maté, J. I. (2008). Effect of the presence of glycerol and Tween 20 on the chemical and physical properties of films based on chitosan with different degree of deacetylation. *LWT - Food Science and Technology*, *41*(10), 2159–2165. https://doi.org/10.1016/j.lwt.2007.11.023

Zink, J., Wyrobnik, T., Prinz, T., & Schmid, M. (2016). Physical, chemical and biochemical modifications of protein-based films and coatings. An extensive review. *International Journal of Molecular Sciences*, *17*(9), E1376.

Supporting Information

Additional supporting information may be found online in the Supporting Information section at the end of the article.

Figure 1: Elongation at break of BLG films in which we incorporated either protein-stabilized SLN (BS) or Tween 20-stabilized SLN (TS). Films without SLN or with the respective emulsifier mixtures E1 (for TS) and E2 (for BS) served as control.

Figure 2: Water sorption of raw material

Figure 3: Loss Modulus as a function of relative humidity of BLG films in which we incorporated either protein-stabilized SLN (BS) or Tween 20-stabilized SLN (TS). Films without SLN or with the respective emulsifier mixtures E1 (for TS) and E2 (for BS) served as control